Energy Proceedings
Vol 38, 2024
ISSN 2004-2965

Experimental investigation of CO_2 flooding in tight oil reservoirs: Effects of the fracture aperture on production characteristics and oil distribution

Mingyang Yang [1], Shijun Huang [1*], Fenglan Zhao [1], Haoyue Sun [1], Xinyang Chen [1], Xinhan Fan [1]

1 College of Petroleum Engineering, China University of Petroleum (Beijing)

(*Corresponding Author: hshj@cup.edu.cn)

ABSTRACT

Field observations, along with experimental laboratory, exhibit evidence that gas injection in tight oil reservoirs is technically feasible. However, there is a lack of understanding the effects of fracture aperture on the oil production behaviors, especially when the fracture aperture is less than 50μm. In this study, CO_2 flooding experiments were carried out using different fracture aperture core samples considering the confining pressure (11μm, 15μm, 20μm, 25μm). And the production characteristics and remaining oil distribution were evaluated based on nuclear magnetic resonance (NMR). The results showed that fracture aperture is of significance to the permeability. Specifically, with the increase of fracture aperture, permeability increases in power law while porosity increases linearly. It is worth noting that the recovery of CO_2 flooding is the highest (17.60%) after water flooding when the fracture aperture is 20μm. Moreover, the dissolution diffusion mechanism becomes more obvious when the fracture aperture increases (10~20μm), but gas channeling will lead to a large amount of remaining oil when the fracture aperture exceeds a certain limit (20~25μm) according to the results of nuclear Magnetic Resonance Imaging (MRI). The results provide a theoretical basis for further understanding the effect of fracture aperture on CO2 injection in tight reservoirs.

Keywords: tight oil reservoirs, CO_2 flooding, fracture aperture, production characteristics, oil distribution

NONMENCLATURE

Abbreviations	
NMR	Nuclear Magnetic Resonance
MRI	Nuclear Magnetic Resonance Imaging
EOR	Enhance Oil Recovery
HnP	Huff and Puff
EGS	Enhanced Geothermal Systems
Symbols	
$Ø$	Porosity, %
$Ø_f$	Fracture porosity, %
K	Permeability, mD
K_f	Fracture permeability, mD
W_f	Fracture aperture, μm
W_{fc}	Fracture aperture (15MPa), μm
A	Core cross-sectional area, cm^2
R	Core radius, cm

1. INTRODUCTION

The effective development of unconventional reservoirs, such as tight and shale reservoirs, is of great significance to the supply of energy due to the depletion of conventional reservoirs[1]. And it is reported that the oil production from tight reservoirs has accounted for more than 50% of US overall oil production in 2018[2]. It is worth noting that the successful application of horizontal drilling combined with volumetric fracturing in unconventional reservoirs makes it possible to develop unconventional reservoirs economically and effectively. But according to the feedback results, the recovery rate of tight oil reservoir is less than 10%[3,4]. This means that a large amount of remaining oil is still untapped underground. Therefore, it is necessary to explore effective ways to enhance oil recovery (EOR)[5]. CO_2 injection has attracted much attention due to its low injection pressure, mass transfer, viscosity reduction and miscibility[6–9]. Meanwhile, CO_2 injection can achieve a reduction in carbon emissions[10,11]. However, the existence of fractures makes the possibility of gas channeling greatly increased during gas injection[12].

In recent years, many researchers have studied the effect of fracture on remaining oil distribution and

This is a paper for 15th International Conference on Applied Energy (ICAE2023), Dec. 3-7, 2023, Doha, Qatar.

recovery. Zhang investigated the effects of fracture length and aperture on the composition, and concluded that fracture length and aperture had a significant effect on the gas phase composition at the outlet, but had little effect on the oil phase composition[13]. Zhou found that the fracture aperture distribution significantly affects Enhanced Geothermal Systems (EGS) performances[14]. Bai studied the effects of fracture on production characteristics and oil distribution during CO_2 HnP, and they found that fractures can reduce the effect of permeability on recovery[15]. Guo employed a novel multiscale-fluidic system to investigate the multiphase transport and phase transition, and demonstrated that fractures help to elevate the bubble point pressure when the matrices and fractures are interdependently coupled[16].

According to the literature, there are few studies focusing on the effect of the fracture aperture on production characteristics and oil distribution, especially when the fracture aperture is less than 100μm. In this study, we conducted CO_2 flooding experiments with different fracture apertures to study the effect of fracture aperture on recovery and remaining oil distribution. This study significantly advances our understanding of the CO2 EOR in fractured reservoirs and holds great potential for guiding practical engineering applications.

2. EXPERIMENTAL

2.1 Materials

The artificial core samples used in the experiments had a diameter of 1 in. In each core sample, different thickness films are pre-arranged to simulate different fracture apertures. The details of the parameters of the cores used in this research are collated in Table 1. The experimental gas includes CO_2 with a purity of 99.9% which is supplied by the Huatongjingke Gas Company, China. The oil sample used for the gas flooding experiments is the dead oil collected from the Changqing Oilfield. Its density and viscosity were measured to be 846.9 kg/m^3 and 5.15 mPa.s (at 75℃ and 0.101Mpa), respectively. The compositional analysis of the dead oil is presented in Table 2. To avoid the influence of the water signal, the water sample used in the experiment is D_2O.

Table 1 Petrophysical properties of the tested cores.

Sample No.	Diameter [mm]	Length [mm]	Fracture aperture [μm]	Porosity [%]	Permeability [mD]
1	25.50	68.73	20	17.87	6.79
2	25.71	64.52	30	19.65	14.42
3	25.52	67.96	40	20.17	35.71
4	25.43	63.74	50	22.49	69.62

Table 2 Compositional analysis results of the oil sample.

Carbon number	Mol. [%]	Carbon number	Mol. [%]
C_1	0	C_{19}	5.86
C_2	0	C_{20}	5.60
C_3	0.07	C_{21}	5.56
C_4	0.53	C_{22}	4.98
C_5	1.08	C_{23}	4.78
C_6	1.56	C_{24}	3.99
C_7	2.12	C_{25}	3.84
C_8	3.04	C_{26}	3.11
C_9	2.84	C_{27}	2.75
C_{10}	3.19	C_{28}	2.03
C_{11}	3.50	C_{29}	1.71
C_{12}	3.80	C_{30}	1.14
C_{13}	4.38	C_{31}	0.92
C_{14}	4.88	C_{32}	0.60
C_{15}	5.33	C_{33}	0.58
C_{16}	4.98	C_{34}	0.33
C_{17}	5.33	C_{35+}	0.25
C_{18}	5.35	/	/

2.2 Apparatus

The experimental apparatus used in this study mainly includes a core holder, a high-pressure ISCO pump (Model 100DX, Teledyne Co., Ltd., USA), temperature, gasometer, circular pump, back pressure regulators, recording system, etc. NMR system was performed to characterize the remaining oil distribution of crude oil in cores. The system was manufactured by Niumag Corporation Ltd. in China. The magnetic field strength is about 0.3±0.05 T. The center frequency is 12 MHz. A schematic diagram of CO_2 flooding apparatus is shown in Fig. 1.

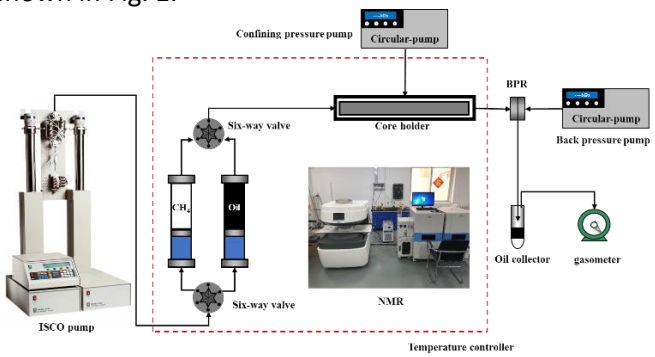

Fig. 1. Schematic diagram of CO_2 flooding apparatus.

2.3 Experimental procedure

The specific experimental steps are as follows:

(1) Saturation: The core holder is heated to 75 °C and the core is pressurized to 15 MPa. Place the core into the core saturation device and vacuum it for 24 hours. Then open the inlet switch, and the oil was injected into the core. NMR test was performed when saturation was completely saturated with oil and aged.

(2) Water flooding: Continue to saturate the crude oil and slowly increase the back pressure to 10 MPa. D_2O is injected into the core at a constant rate of 0.2 ml/min, then the liquid at the output end is collected and the pressure changes of the injection end and the output end are monitored.

(3) CO_2 flooding: When the water cut is about 99%, gas injection is started at 0.2 ml/min at constant speed until the core is no oil produced. Record the change of liquid yield and pressure during the process of flooding. And the confining pressure was ensured to be 15 MPa during the experiments. At last, NMR test was performed to clarify the distribution of remaining oil.

3. RESULTS AND DISCUSSION

3.1 The relationship between fracture aperture and petrophysical properties of the cores

According to the equivalent seepage theory, the relationship between fracture permeability and fracture aperture is shown in Equation (1). Fracture porosity is shown in Equation (2).

$$K_f = 1000\phi_f {W_f}^2/12 \quad (1)$$

$$\phi_f = RW_f/10000A \quad (2)$$

The relationship between fracture aperture and fracture permeability can be deduced by combining Equation (1) and Equation (2), as shown in Equation (3).

$$W_f = \sqrt[3]{120AK_f/R} \quad (3)$$

Since the core matrix permeability is low, we assume that the fracture permeability is consistent with the permeability obtained experimentally in Table 2. Therefore, the fracture aperture under confining pressure (15MPa) can be obtained by Equation (3), as shown in Table 3. The pressure has an important influence on the fracture aperture. Specifically, the fracture aperture is reduced by half under the confining pressure of 15MPa.

Table 3 Fracture aperture of different cores

Sample No.	W_f [μm]	W_{fc} [μm]
1	20	11
2	30	15
3	40	20
4	50	25

As shown in Fig. 2, the fracture aperture has an important effect on the basic physical properties of the core including permeability and porosity. Moreover, the relationship between permeability and fracture aperture is power law, while the relationship between porosity and fracture aperture is close to linear, as shown in Equation (4) and (5). At the same time, it can be seen that the correlation coefficients are both larger than 0.94. This finding proves that fractures are important seepage channels in tight reservoirs.

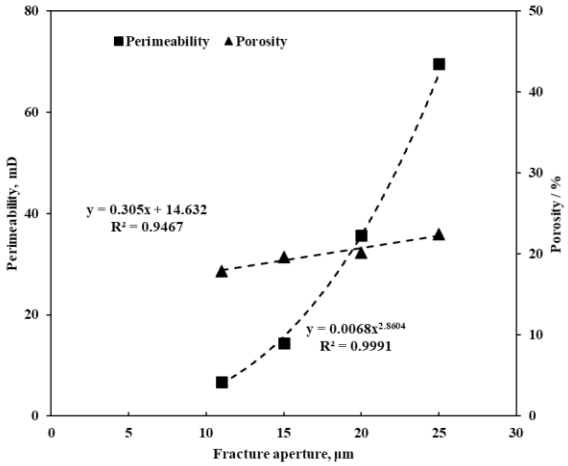

Fig. 2. Permeability and porosity in the experimental core samples with different fracture aperture.

$$\phi = (0.305 * W_f + 14.632)/100 \quad (4)$$

$$K = 0.0068 * {W_f}^{2.8604} \quad (5)$$

3.2 The recovery of the cores with different fracture aperture

Fig. 3 shows the recovery of the water flooding and CO_2 flooding for the cores with different fracture apertures. It can be found that with the increase of injection volume, the recovery increases rapidly at first and then tends to be stable gradually in the process of water flooding. It is worth noting that the water flooding recoveries of water flooding are 41.63%, 46.73%, 48.21%, 36.73% when the fracture aperture is 11μm, 15μm, 20μm, and 25μm, respectively. Moreover, recovery of CO_2 flooding for the cores with different fracture apertures also shows the same trend, as shown in Fig. 4. This indicates that the injection medium is more likely to break through When the crack opening is more than 20 μm.

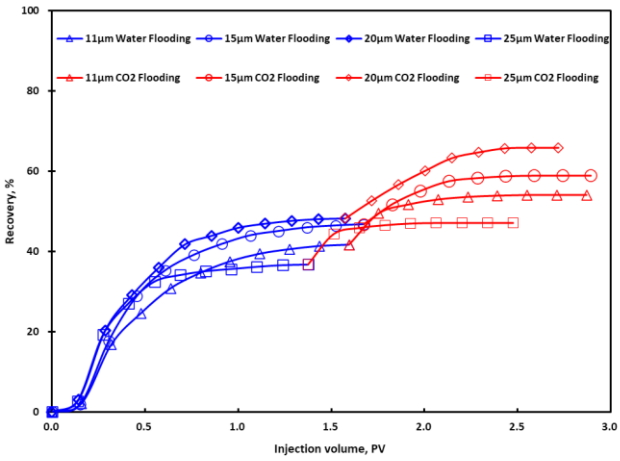

Fig. 3. Recovery of cores with different fracture apertures.

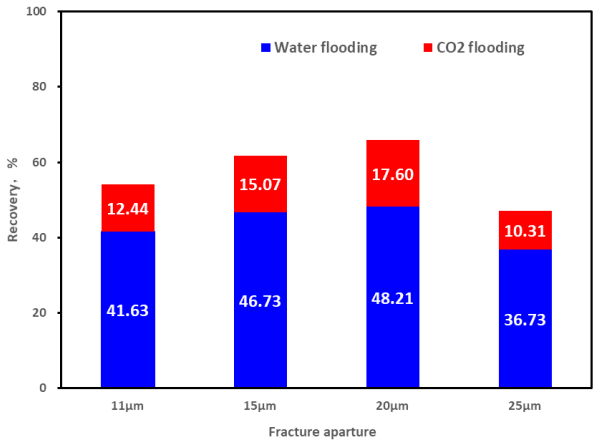

Fig. 4. Recoveries of water flooding and CO_2 flooding in cores with different fracture apertures.

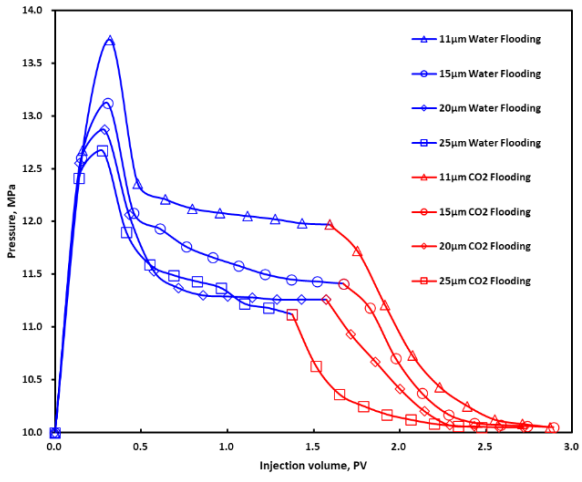

Fig. 5 Pressure variation during water and CO_2 flooding of cores with different fracture apertures.

Fig. 5. shows that the injection pressure decreases gradually in the process of water flooding with the increase of fracture aperture. At the beginning of gas flooding, the rapid decrease of injection pressure reflects the lower injection pressure of gas. However, higher injection pressure causes CO_2 to invade from the fracture to the matrix, which makes more oil near the fracture to be squeezed into the matrix. This invasion mechanism is often ignored, but it is a fact that the convection effect is much greater than the mass transfer in the displacement process due to the limitation of interaction time. As shown in Fig. 6, the water breakthrough time is advanced and the water cut increases rapidly after water breakthrough with the increase of fracture aperture. The rapid increase of water cut is an important reason for the low recovery of water flooding for the core fracture aperture with 25 μm. And the variation of water cut is the same when the fracture aperture is less than 20 μm.

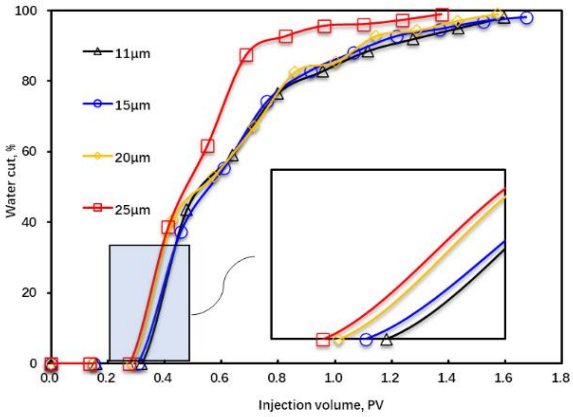

Fig. 6. Water cut during water flooding.

Fig. 7 shows the change in gas oil ratio during gas flooding. And it can be found that the gas oil ratio of the core with the fracture aperture is 20 μm is lower than the others. This is mainly because the diffusion mass transfer between fracture and matrix is more obvious when the crack opening is 20 μm.

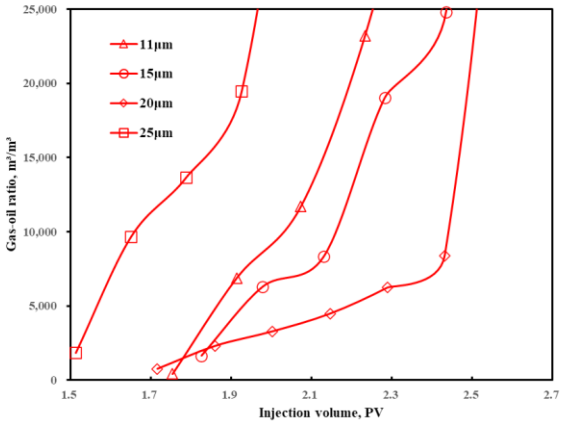

Fig. 7. Gas oil ratio during gas flooding.

3.3 Effect of different fracture aperture on remaining oil distribution

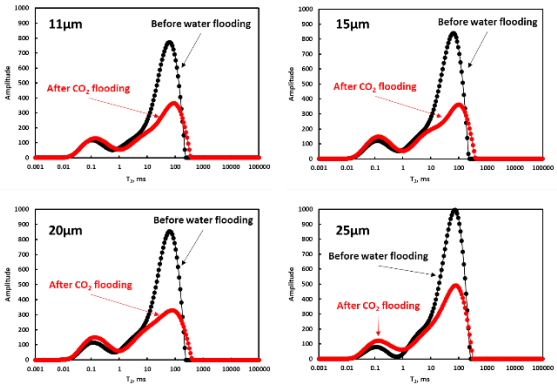

Fig. 8. T_2 spectrum of cores with different fracture apertures.

Fig. 8 shows T_2 spectral curves of the core samples by the NMR during the process of water and CO_2 flooding. The bimodal peaks of T_2 spectral curve at saturation indicate that there are mainly two kinds of pore structure in the core. And the amplitude of the right peak is higher, which indicates that large pores are dominant. It can be found that the signal of the core sample increases with the increase of fracture aperture. This is mainly due to the increase in the fracture volume. Compared with the T_2 spectrum curve before and after displacement, the crude oil mainly comes from macropores (T_2 > 10ms). However, it is evident that the distribution of remaining oil in cores with different fracture aperture is different, as shown in Fig. 9. This indicates that fracture aperture is of significance to the production characteristics and oil distribution. It can be found that the residual oil in the core with a fracture aperture of 25 μm is the most, and the crude oil in the fracture is mainly recovered. However, the remaining oil is mainly distributed around the fracture and at the outlet of the core when the fracture aperture is 11 μm and 15 μm. This is mainly because of the diffusion mass transfer caused by the concentration difference between the fracture and the matrix. In addition, the decrease of pressure during gas injection can also cause part of the crude oil in the matrix to flow into the fracture. At the same time, there is less residual oil in the fracture at the entrance of the core, which may be caused by the formation of oil-water slug at the fracture position at the exit of the core, causing the injected CO_2 to bypass the fracture and unlock the crude oil in the matrix around the fracture. When the fracture aperture is 11 μm, the residual water in the fracture will increase the resistance of gas entering the fracture. Thus, the injected gas has a higher probability of entering the matrix for oil production.

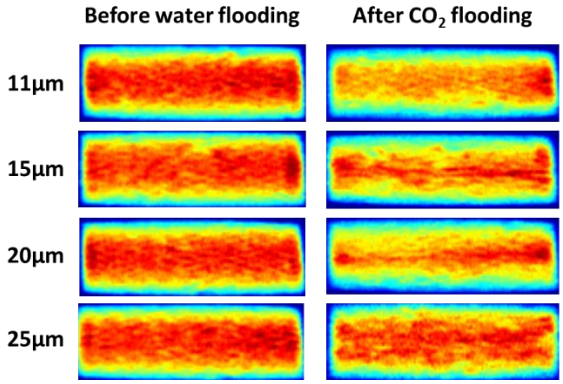

Fig. 9. The oil distribution after CO_2 flooding in the core samples with different aperture.

4. RESULTS

In this study, the relationship between petrophysical properties of the cores and fracture aperture was discussed. At the same time, the effect of the fracture aperture on recovery was proposed based on the CO_2 flooding experiments. Moreover, the difference in production characteristics and oil distribution is explained based on NMR. The main conclusions of this work are as follows:

(1) The effect of fracture aperture on permeability is far greater than that on porosity. The permeability has a power law relationship with the fracture aperture, while the porosity increases linearly with the fracture aperture.

(2) The oil recovery of water flooding and CO_2 flooding is obviously decreased when the fracture aperture is over 20 μm. The main reason is that the larger fracture aperture will lead to the early breakthrough of injection media, so it can not unlock more oil effectively.

(3) When the fracture aperture is small, the residual water formed in the fracture after water flooding will form slug with injected gas, which helps enhance oil recovery. At the same time, the rapid pressure drop during gas injection will cause the oil in the matrix to flow to the vicinity of the fracture.

ACKNOWLEDGEMENT

The research is financially supported by the National Natural Science Foundation of China (52174039) and the National Natural Science Foundation of China (51974328).

DECLARATION OF INTEREST STATEMENT

The authors declare that they have no known competing financial interests or personal relationships that could have appeared to influence the work reported in this paper. All authors read and approved the final manuscript.

REFERENCE

[1] Wang J, Feng L, Steve M, Tang X, Gail TE, Mikael H. China's unconventional oil: A review of its resources and outlook for long-term production. Energy 2015; 82: 31–42.

[2] Alfarge D, Wei M, Bai B. IOR Methods in Unconventional Reservoirs of North America: Comprehensive Review, OnePetro; 2017.

[3] Ren B, Ren S, Zhang L, Chen G, Zhang H. Monitoring on CO2 migration in a tight oil reservoir during CCS-EOR in Jilin Oilfield China. Energy 2016; 98: 108–21.

[4] Alharthy N, Teklu T, Kazemi H, Graves R, Hawthorne S, Braunberger J, et al. Enhanced Oil Recovery in Liquid–Rich Shale Reservoirs: Laboratory to Field. SPE Reservoir Evaluation & Engineering 2017; 21: 137–59.

[5] Wei B, Liu J, Zhang X, Wang D, You J, Lu J, et al. Dynamics of mass exchange within tight rock matrix/fracture systems induced by natural gas 'dynamic' soaking and oil recovery prediction. Energy 2022; 254: 124331.

[6] Wang L, Wei B, You J, Pu W, Tang J, Lu J. Performance of a tight reservoir horizontal well induced by gas huff–n–puff integrating fracture geometry, rock stress-sensitivity and molecular diffusion: A case study using CO2, N2 and produced gas. Energy 2023; 263: 125696.

[7] Zuloaga P, Yu W, Miao J, Sepehrnoori K. Performance evaluation of CO2 Huff-n-Puff and continuous CO2 injection in tight oil reservoirs. Energy 2017; 134: 181–92.

[8] Tang W-Y, Sheng JJ, Jiang T-X. Further discussion of CO2 huff-n-puff mechanisms in tight oil reservoirs based on NMR monitored fluids spatial distributions. Petroleum Science 2022.

[9] Hashemi SMH, Sedaee B. Mechanistic simulation of fracture effects on miscible CO2 injection. Petroleum Research 2022; 7: 437–47.

[10] Chen P, Bose S, Selveindran A, Thakur G. Application of CCUS in India: Designing a CO2 EOR and storage pilot in a mature field. International Journal of Greenhouse Gas Control 2023; 124: 103858.

[11] Lv Q, Zheng R, Zhou T, Guo X, Wang W, Li J, et al. Visualization study of CO2-EOR in carbonate reservoirs using 2.5D heterogeneous micromodels for CCUS. Fuel 2022; 330: 125533.

[12] Cao A, Li Z, Zheng L, Bai H, Zhu D, Li B. Nuclear magnetic resonance study of CO2 flooding in tight oil reservoirs: Effects of matrix permeability and fracture. Geoenergy Science and Engineering 2023:211692.

[13] Qing-Fu Z. Laboratory investigation of the influence of fractures on CO2 flooding. Frontiers in Earth Science 2022;10.

[14] Zhou D, Tatomir A, Tomac I, Sauter M. Effects of fracture aperture distribution on the performances of the enhanced geothermal system using supercritical CO2 as working fluid. Energy 2023; 284: 128655.

[15] Bai H, Zhang Q, Li Z, Li B, Zhu D, Zhang L, et al. Effect of fracture on production characteristics and oil distribution during CO2 huff-n-puff under tight and low-permeability conditions. Fuel 2019; 246: 117–25.

[16] Guo Y, Shi J, Qiu J, Xu Z, Bao B. Visualized investigation of transport and phase behaviors during CO2 huff-n-puff in nanomatrix-fracture tight formations. Fuel 2023; 354: 129344.